A Hybrid Nanomofs Based Power Generation System

Sara Shahmohammadi[1], Alexander Burns[2], Boyd Davis[3]

[1]Hybrixcel Inc., [2]NORAM Engineering Ltd., [3]Kingston Process Metallurgy Inc.

[1]sara.shahmohammadi@hybrixcel.com

ABSTRACT

The moonshot challenge of our future is to meet the soaring demand for energy needs and to protect our climate at the same time. Fossil fuels are limited resources; hence there will be need for more renewable energy as well as more efficient use of energy by recovering alternative sources. There is a significant amount of low temperature geothermal and waste heat generated in the world costing the economies billions and causing environmental damage. This heat cannot be effectively utilized using currently available technologies due to their limitations of cost, size, complexity of integration with other energy sources and the need for high operating temperature. This paper investigates the potentiality of applying technology of fluidized bed to temperature/pressure swing adsorption (TSA/PSA) processes employing certain commercial sorbents, nominally a metal-organic framework (MOF), to adsorb and desorb fluorocarbon refrigerants to improve heat and mass transfer in a power generation system. The overarching purpose of the system is to convert low to mid-grade heat into electricity and introduce a breakthrough new thermodynamic cycle. Different cycle layouts and configurations identified for a possible refrigerant-sorbent pairs for potential inclusion in the present work and were simulated in Aspen Adsorption to perform respectively the balance of plant and a detailed fluidized bed design. Four main scenarios to assess the impact on overall system design, performance and costs, were modelled and compared. The results reveal a neat superiority of fluidized-bed over fixed-bed in terms of both performance and efficiency.

1. INTRODUCTION

As population has grown significantly during last century, millions of people who live in developing countries still lack to access to secure electricity grids and thus using conventional fossil fuels have a negative impact on the environment issues such as global warming and the climate change which pushed more research towards a real change in the energy policy [1]. Also, energy intensive industries face strong challenges due to rising electricity costs and environmental limitations; therefore, developing methods for energy efficiency improvement is becoming an increasingly important issue. Despite significant efforts have been directed toward solutions to improve industrial energy efficiency, the average energy efficiency is 49%, with 30% of the energy input rejected as waste heat, mostly as low to mid-grade waste heat (42% of the total) [2]. In U.S., this amounts to approximately 68.5 quads of wasted thermal energy according to an energy flow chart released by Lawrence Livermore National Laboratory in 2018. In U.S. geothermal resources at temperatures less than 150 C. represent an additional very large (100 GWth) and widely geographically dispersed resource. One of the challenges of geothermal energy is that it does not provide very high temperatures, and this fact has made researchers and engineers to focus their studies on how to obtain high thermodynamic efficiencies at low- and medium-temperature heat sources.

Historically, the preferred methods for power generation have been related to Brayton or Rankine power cycles, fuelled by natural gas or other fossil fuels [3].

The efficiency of standard thermodynamic cycles such as the Rankine cycle are inherently low, less than 10% typically resulting high capital and operating costs relative to the amount of revenue that can be generated from power sales is rarely very economically attractive, especially today with low costs for natural gas. Hence there is a pressing need for new concepts that can dramatically bend the cost curve of power production from low grade heat sources. Thermally driven ORC systems in heat conversion systems based on the reversible adsorption and desorption of the working fluid that apply porous adsorbent materials are very promising. Thus, the more efficient use of low-temperature heat and an effective adsorption approach, as well as effective climate protection through the reduction of the environmental impact of conventional technology, is encouraging [4-6].

In our study, we carried out a numerical modelling of both a standard ORC system and a reference case system introduced by Jenks et al. [6], so called HARP that uses the chemical adsorption in affinity of new nanostructured porous materials in a fixed-bed thermal compressor that eliminates the evaporator, condenser, and high pressure pump in the standard ORC. Based on our investigations, we found that the main disadvantage of the fixed-bed adsorption system is low coefficients of performance (COP) and how system suffers from two main drawbacks: (1) a great amount of the energy must be accounted for the heating and cooling of the bed, and (2) a large footprint is required to process large flow rates. One of the well-known methods allowing to improve (COP) widely used in energy boilers is using fluidized bed [7]. Thus, through a process modelling and simulation, focused on the optimization of the cycle, we decided to design a fluidized bed in place of the fixed bed, as an alternative leading to increase of the adsorption and desorption processes which overcomes the inherent limitations of the reference case system. Although fluidized beds represent an already established technology and are extensively employed in a wide variety of industrial processes since the beginning of the last century, combining adsorption with the fluidization of the sorbent is a recent proposal. The concept of using a fluidized bed to enhance the performance of an adsorption chiller was published by Wang et al. (2012) [8].

2. ORGANIC RANKINE CYCLE

The basic Organic Rankine cycle (ORC) can be powered by a low-grade heat sources such as geothermal energy or waste heat and it has four main processes. During process 1–2 the refrigerant liquid will be pumped to the evaporator pressure, while through process 2–3 heat is added to the evaporator from an external source (low grade heat source). During, 3–4 the refrigerant expands through an expander (turbine) where the mechanical power can be produced and finally, through 4–1 the refrigerant is cooled in the condenser [9]. This is the simplest ORC, which can be seen in Figure 1, together with a typical P-h diagram for the same cycle layout. This simple configuration can be modified to obtain higher efficiencies.
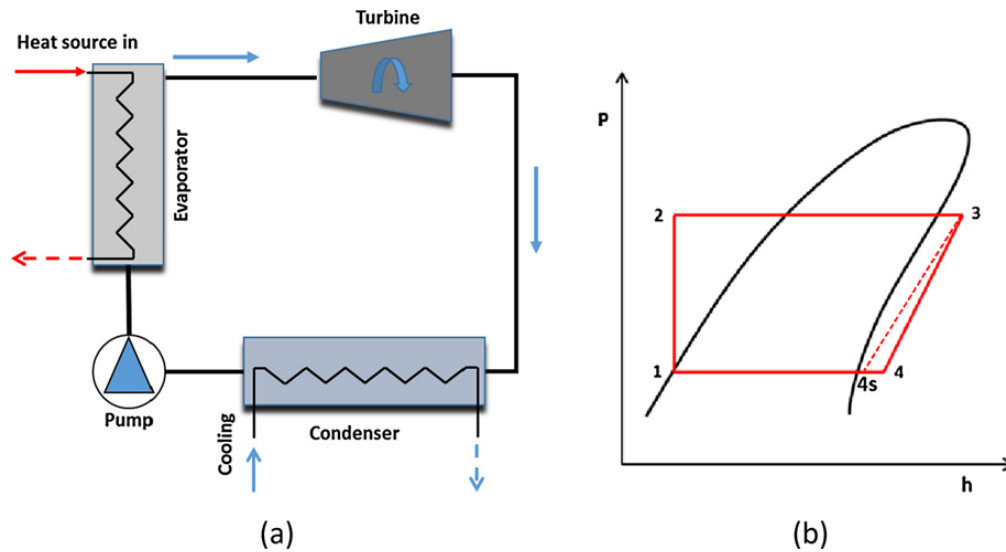

Figure 1. Simple ORC layout for a random pure working (a) schematic diagram and (b) P-h diagram.

3. ADSORPTION COOLING SYSTEM

Figure 2a shows a schematic diagram of a basic two-bed adsorption cooling system which consists of desorber, adsorber, condenser and evaporator. As the adsorption is an exothermic process a cooling source is used to extract heat from the adsorbent sustain cooling through adsorption process which helps to desorb the refrigerant from the evaporator and generate the cooling effect. Desorption is an endothermic process, and a heat source (low grade heat source) is used to sustain heating during this process which helps to discharge the refrigerant (water vapor) from the hot bed. Then, the hot refrigerant will be cooled in the condenser to feed the evaporator with the refrigerant liquid and keep continuous cooling through the system.

Figure 2b shows the adsorption basic cycle on a P-T diagram; process 1-2 is an adsorbent isosteric heating where a low grade heat source is used and this heating is still continuous during the process 2-3' while the valve 4 is opened, meanwhile a cold source is used during the process 3'-4' and this cooling is still continuous during the process 4'-1 while the valve 2 is opened.

An adsorption system usually consists of two or four beds [10,11]. When some of the beds work as adsorbers, the desorption process occurs in other beds at the same time, and on the contrary. To increase the efficiency of the unit, the beds must be properly prepared for the upcoming phase. Therefore, before the two main stages (i.e. adsorption and desorption) starts the beds previously must be pre-heated (before desorption) or pre-cooled (before adsorption), respectively. During these short periods, usually called switching time periods, all valves connecting the beds with the evaporator and the condenser are closed. By this way, four phases: pre-cooling, adsorption, pre-heating and desorption, occur one by one during the full adsorption cooling cycle in each of the bed of an adsorption system.

3.1 TSA/PSA Processes in Fluidized Bed

When solid sorbents are employed in a large scale process, the regeneration step is commonly performed by means of either pressure swing adsorption (PSA) or temperature swing adsorption (TSA) cycles, in which the thermodynamic properties of the solids are manipulated by changing the pressure or temperature levels of the system, respectively. In addition, the two different routes can be combined when designing a cycle, so as to maximize the efficiency of the sorbent regeneration for given temperature and pressure ranges. The simplest system for heat capture via adsorption consists of two separated fluidized bed reactors, one for the adsorption stage and one for the regeneration phase.
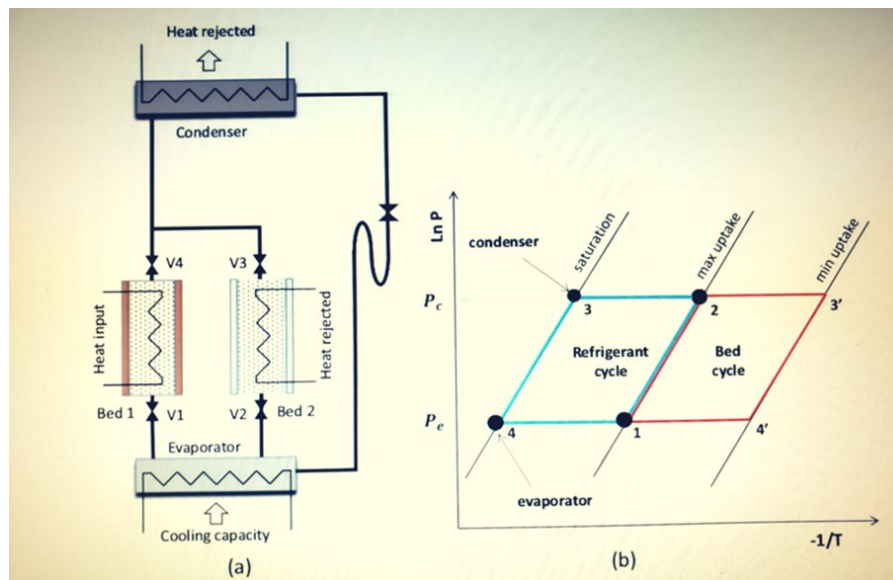
Figure 2. **A basic two-bed adsorption cooling (a) schematic diagram and (b) P-T diagram.**

4. OPERATING CYCLE

The central unit operation to the system is a four identical adsorption and desorption bed carousel. Each bed is rotated through a sequence of four steps:

1. Unloaded and pre-cooling – The adsorption bed has just been discharged of its refrigerant and is in the unloaded state. The bed is taken to lower pressure and pre-cooled. This step mainly serves to lower the temperature of the solids in the bed and associated equipment (sensible heat) in anticipation of step 2.
2. Unloaded and adsorbing – The sorption bed adsorbs working fluid from the discharge of the turbine. It operates in the lower-pressure state. The sorption bed effectively performs the same function as a condenser in a traditional refrigerant cycle, but instead of transitioning from gas to liquid, the refrigerant transitions from gas to an adsorbed state. The adsorption is exothermic, so this step continues to reject heat to the heat sink until the bed reaches a predetermined loading level or a certain length of time has elapsed.
3. Loaded and preheating – The loaded sorbent bed is pre-heated and allowed to start building pressure. This step mainly serves to raise the temperature of the solids in the bed and associated equipment sensible heat), but also to begin to build up pressure in anticipation of step.
4. Loaded and discharging – The sorption bed acts to generate pressure and flow to feed the turbine. Unlike a traditional compressor, where mechanical energy is used to build pressure, the input of heat causes refrigerant to desorb from a sorbent, which releases gas and maintains pressure in the process. The pressurized gas is released through an automatically sequenced valve to perform mechanical work in a downstream turbine. This step continues to accept heat from the heat source until the bed declines to a predetermined loading level.

The temperature and pressure inside each bed is dynamic, and as such the pressure at the discharge of the carousel (that feeds the turbine) fluctuates.

5. FLUIDIZATION CHARACTERISTICS

5.1 Particle characteristics

Fluidization behaviour of spherical particles is strongly dependent on particle diameter and density. Larger, denser particles have higher terminal velocities, and also higher minimum fluidization velocities. This means they require more energy to fluidize. However, very small and low density particles exhibit other challenging fluidization behaviour – the electrostatic forces between the particles becomes dominant over drag, which leads to channelling and poor fluidization as the particles adhere to one another. These challenges can be overcome by use of special methods, such as high velocity gas jets, pulsating flow, and mechanical vibration of the beds. However, this usually leads to fluidization of more uniform agglomerates rather than true fluidization of nanoscale particles.

For conventional fluidization techniques, Geldart researched different powders and proposed a fluidization chart (reproduced below from (Richardson, Harker, & Backhurst, 2002))
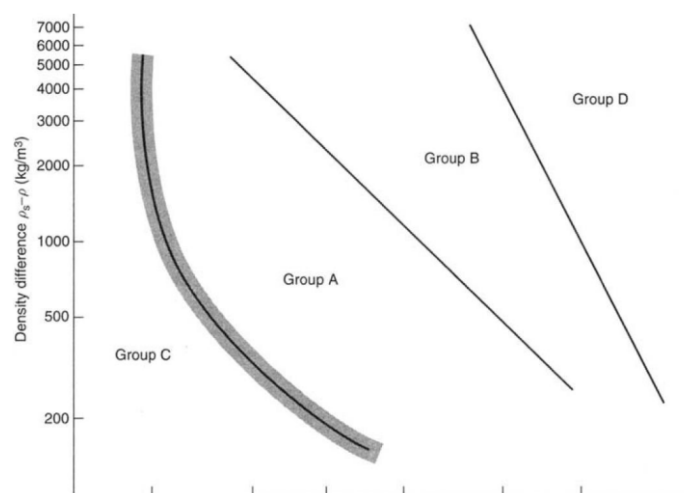
Figure 3. Fluidization regimes depending on particle size and density difference. Source: Richardson, Harker, & Backhurst, 2002.

For this system, it will be desirable to use a material which can be processed into a Group A solid. This will allow stable fluidization over a good range of velocities and conditions as the conditions in the bed change through the charge and discharge cycle. Other important characteristics of the solid are a tight particle size distribution, and a high resistance to attrition. If there is a wide range of particle sizes, the system will suffer problems with entrainment of the finer particles into the turbine. If the particles are friable (susceptible to attrition through the mechanical action between particles in the fluid bed) then they will not last long in service before they require replacement.

It is expected that developing an adsorbent material with these properties will be a substantial challenge in the technology development pathway from concept to commercial implementation of fluidized beds in this service.

5.2 Energy required for fluidization

Energy is expended in order to maintain the beds of solids in a fluidized state. Once fluidization has been attained, the pressure drop over a bed of solids is independent of the gas velocity until terminal velocity is reached. The pressure drop is equal to the mass of suspended solids per unit cross sectional area of the bed. Therefore, the energy required to fluidize a bed of solids is equal to the weight of the bed times the superficial velocity of fluidizing gas, divided by the circulation blower efficiency.

Refrigerant adsorbed onto the solids contributes to the weight of solids being fluidized. This changes during the charge / discharge cycle of each bed, but the mass of adsorbent that exists in adsorbed state in the entire system is fairly constant. Using the typical loading swing considered in previous work (by PNNL) of 50 – 130 wt% adsorbed, the total mass of adsorbed refrigerant in the system is equal to the mass of sorbent multiplied by 90%. This is broadly consistent with the loadings predicted in the present work.

The circulation blower efficiency is given arbitrarily as 30% (typical of air handling equipment). The superficial velocity in the bed will be some multiple of the minimum fluidization velocity, which can be calculated as a function of gas and solid physical properties. Assuming a voidage of 0.4 at incipient fluidization, minimum fluidization velocity can be estimated (Richardson, Harker, & Backhurst, 2002) as:

$$Umf = 0.00059 \; d2(\rho s - \rho g) \; g/\mu g$$

Assumptions for the calculations include: an adsorbent with a stable particle size of 50 microns; a particle solids density of 620 kg/m3; zero volume change on adsorption; a density of the particles in the discharged state (50 wt. % loaded) of 930 kg/m3; and the density of the particles in the charged state (130 wt% loading) of 1430 kg/m3.

Using R134A as the refrigerant, Umf can be assessed at the two pressure extremes of the charged and discharged states. The calculated range of minimum fluidization velocity is 1.0 to 1.1 mm/s. Note that increasing the particle diameter by a factor of 10 increases required velocity for minimum fluidization by a factor of 100. For uniform fluidization assume a minimum of 10 x Umf. Therefore, a superficial velocity of 11 mm/s is selected.

The mass of sorbent required is dependent on the achievable refrigerant loading, the number of beds, and the cycle time.

5.3 Type of fluidized bed

Two types of fluidized bed have been considered: bubbling bed or circulating bed. Heat and mass transfer are typically higher in a circulating bed. However, this is accompanied by substantial entrainment of the solids in the gas stream, which must then be captured in a cyclone or series of cyclones and returned to the bed. The higher velocity required for a circulating bed also results in more attrition, which in this case would be undesirable. Maintaining a higher velocity also consumes more energy than a lower-velocity bubbling bed. The results reveal that a bubbling bed also requires less energy, and thus imposes a lower parasitic load on the power generation cycle.

5.4 Development of an isotherm model

The amount of refrigerant that loads onto a solid adsorbent depends on temperature and pressure. In this system, loading increases at lower temperature and higher pressure and it decreases at higher temperature and lower pressure. Loading data must be collected experimentally in the laboratory. In the present work the data published by other researchers were used.

Loading isotherms (a mathematical model) are required in order to construct a simulation of the proposed process. Loading data for the R134A/ MIL-101(Cr) system were published by Zheng et al. (2019) over the range of 15 to 35 °C and 0 to 5 bar (a). These data fitted using the temperature-dependent Langmuir model, where w_i is loading in kmol/kg, P_i is the partial pressure of the refrigerant in bar (a), T is temperature in K, and IP_x are independent fitting parameters. The isotherms were extended to higher temperature (90 °C and 200 °C) using the Clausius-Clapeyron relationship, which predicts the known thermodynamic data to different temperatures based on the measured heat of adsorption. Figure 1 shows the raw data and fitted model, and Figure 2 show the same model extended to 30 bar (a), where the proposed process may operate.

$$w_i = \frac{IP_1 e^{IP_2/Ts} P_i}{1 + IP_3 e^{IP_4/Ts} P_i} \quad \text{(partial pressure)}$$
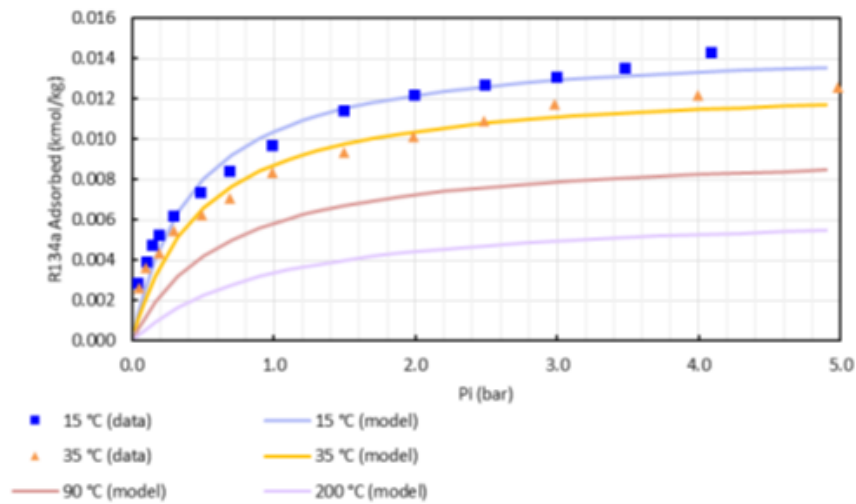

Figure 4. R134a loading on MIL-101(Cr). Data from Zheng et. al. (2019), fit to Langmuir temperature-dependent isotherm model.
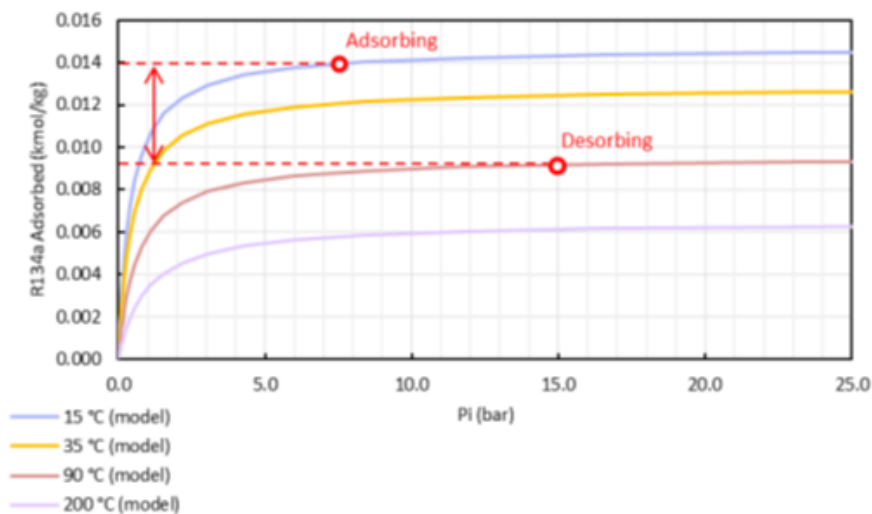

Figure 5. Langmuir model, extended to 20 bar (a), and showing one possible combination of adsorbing/desorbing conditions. Dashed line and arrow added to show the maximum (equilibrium) swing in adsorption across the cycle.

6. PROCESS SIMULATION

A model of the proposed system was constructed in Aspen Adsorption V11. A screen shot of the flow sheet is shown in Figure 6. The model consists of the following blocks:

- Four identical beds consisting of a packed column *Cn* with internal heat exchangers, two empty heads *Cn_HEAD_IN* and *Cn_HEAD_OUT*, inlet valve *VFn* and discharge valve *VPn* arranged in parallel.
- Inlet buffer vessel *TF*.
- Outlet buffer vessel *TP*.
- System inlet valve *VF* (always open).
- System discharge valve *VP* (always open).
- Pipes S1, S2, … S10.
- "Cycle organizer" that sets the valve positions and heat exchange fluid temperature according to a pre-programmed sequence.
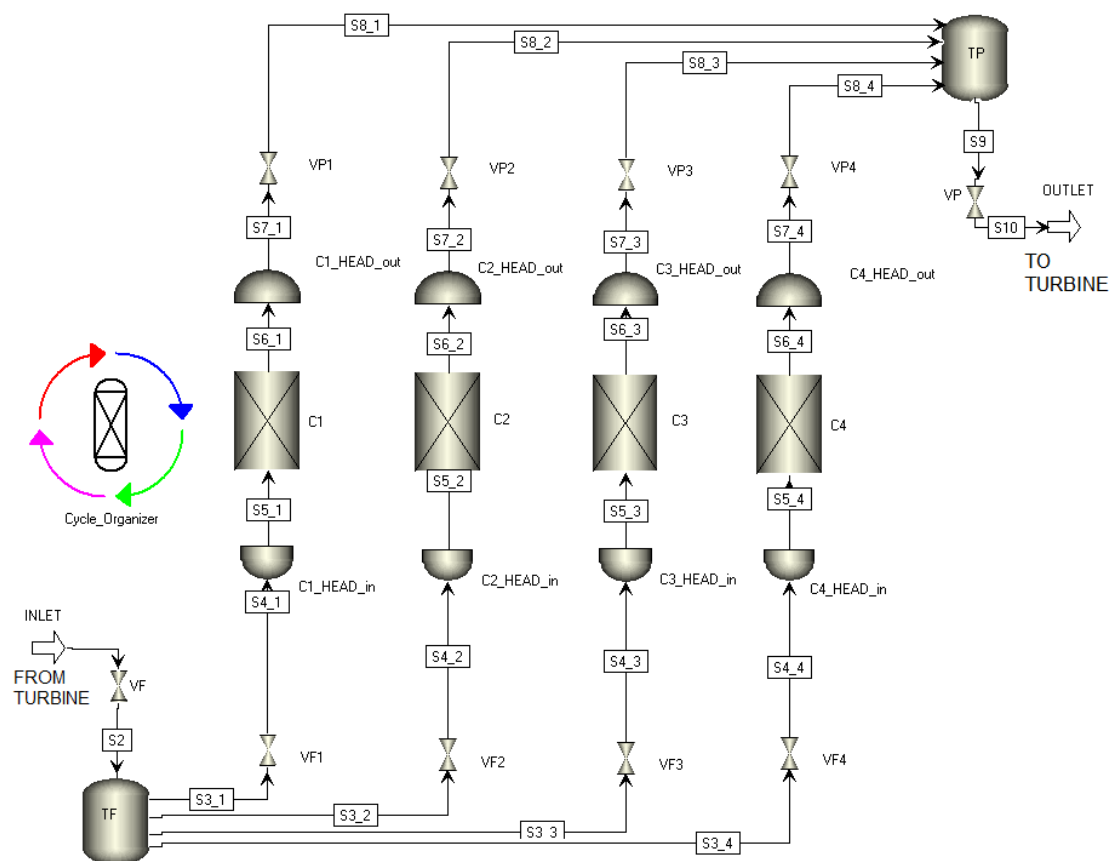
Figure 6. Flow sheet of the system constructed in Aspen Adsorption V11.

The system was modelled as an adiabatic system (no heat transfer into or out of the system). The thermal capacity of the equipment will be added in the future to refine the understanding of heat flow in the system.

The parameters entered into Aspen Adsorption to represent a single bed are given in Figure 6. The physical properties of the refrigerant (R134a) required by the simulation were generated using the Aspen Properties database. The physical properties of the adsorbent (MIL-101(Cr) or NU-1000) were entered manually based on design criteria. The heat and mass transfer coefficients were entered based on the analysis approach, with the actual mass and heat transfer rates calculated by the software based on instantaneous process conditions. Internal bed heat and mass transfer coefficients were set very high to represent the characteristics of a fluidized bed (i.e. uniform gas composition and temperature throughout the bed). Temperature-dependent loading isotherms were entered as described above. The column diameter and height were adjusted to match the size of the system being modelled.

A particle size of 50 micron was assumed. Given that the rate-limiting step appears to be heat transfer between the heat exchanger and the bed, and not mass and heat transfer to the adsorbent particles, there is not likely a benefit to using particles smaller than 50 micron.

The specific surface area defined by design criteria is 1300 m^2/g, which at a density of 250 kg/m^3 converts to 3.25E8 m^{-1}. The maximum value allowable by Aspen Adsorption is 78000 m^{-1}. Given that the system is expected to be heat transfer limited, not mass transfer limited, this discrepancy should not affect the results.
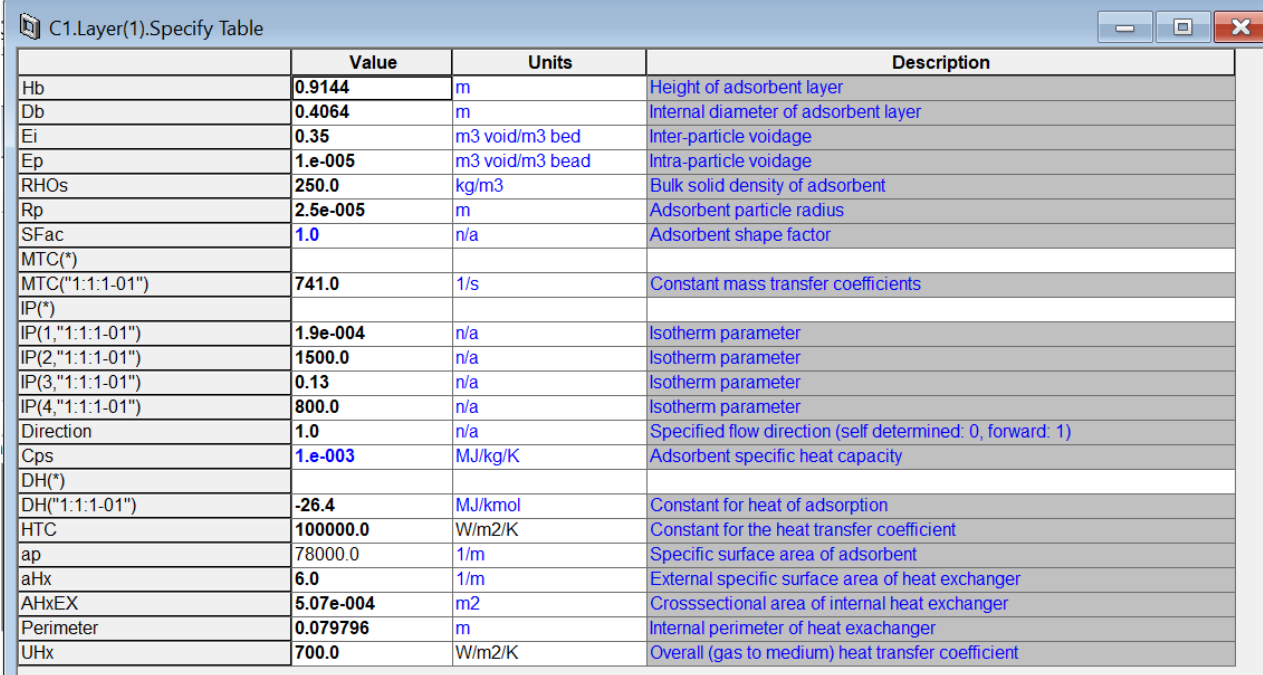
The mass transfer coefficient was assumed to be constant, which is reasonable for a fluidized bed. Selecting a value of 0.0095 m/s and multiplying by the specific surface area of 78,000 m^{-1} gives a value of 741 s^{-1}. This is very fast compared to heat transfer, giving the expected outcome that mass transfer is not limiting in this system.

The heat transfer coefficient of 700 W/m^2. K was chosen based on the earlier analysis of heat transfer in a fluidized bed. Note that this is significantly higher than a non-fluidized system and represents the main advantage of employing a fluidized bed in this system. The actual heat transfer coefficient in a real system may be significantly lower, and this should recognize as a significant uncertainty that needs to be validated.

The heat transfer area is defined in Aspen Adsorption as a "specific surface area" *aHx*, which is the ratio of surface area to bed volume (m^{-1}), as well as parameters for cross-sectional area and perimeter that represent the shape. In this model we have assumed tubular exchangers 1" diameter. *aHx* can vary dramatically depending on the design of the heat exchanger. Along with the heat transfer coefficient, the amount of heat transfer area is critically important in this system.

The switching of each bed between each of the four steps was simulated using Aspen Adsorption's Cycle Organizer feature. The end of each step in the cycle was triggered when the pre-heating bed reached 16 bar (a), which is slightly above the turbine inlet pressure. The temperatures of the heat source / heat sink (*Taux*) fed to each bed were sequenced to simulate the switching of each bed between the heat source and heat sink fluids in a counter-current arrangement.

The height/diameter of the column and heat exchange area *aHX* was adjusted until reasonable temperature differentials, refrigerant flows, and overall performance were achieved for each case. The cycle time was allowed to vary in order to maintain consistent pressures at the discharge. Each simulation was re-run multiple times until the system displayed steady, repeatable performance.

C1.Layer(1).Specify Table

	Value	Units	Description
Hb	0.9144	m	Height of adsorbent layer
Db	0.4064	m	Internal diameter of adsorbent layer
Ei	0.35	m3 void/m3 bed	Inter-particle voidage
Ep	1.e-005	m3 void/m3 bead	Intra-particle voidage
RHOs	250.0	kg/m3	Bulk solid density of adsorbent
Rp	2.5e-005	m	Adsorbent particle radius
SFac	1.0	n/a	Adsorbent shape factor
MTC(*)			
MTC("1:1:1-01")	741.0	1/s	Constant mass transfer coefficients
IP(*)			
IP(1,"1:1:1-01")	1.9e-004	n/a	Isotherm parameter
IP(2,"1:1:1-01")	1500.0	n/a	Isotherm parameter
IP(3,"1:1:1-01")	0.13	n/a	Isotherm parameter
IP(4,"1:1:1-01")	800.0	n/a	Isotherm parameter
Direction	1.0	n/a	Specified flow direction (self determined: 0, forward: 1)
Cps	1.e-003	MJ/kg/K	Adsorbent specific heat capacity
DH(*)			
DH("1:1:1-01")	-26.4	MJ/kmol	Constant for heat of adsorption
HTC	100000.0	W/m2/K	Constant for the heat transfer coefficient
ap	78000.0	1/m	Specific surface area of adsorbent
aHx	6.0	1/m	External specific surface area of heat exchanger
AHxEX	5.07e-004	m2	Crosssectional area of internal heat exchanger
Perimeter	0.079796	m	Internal perimeter of heat exachanger
UHx	700.0	W/m2/K	Overall (gas to medium) heat transfer coefficient

Figure 7. Example of column specifications used for the Aspen Adsorption simulation. Parameters shown are for one of the four defined Scenarios.

7. SIMULATION SCENARIOS

In this paper, the proposed system was simulated under four main scenarios:

1: Low temperature geothermal, commercial scale.

2: Medium temperature geothermal, commercial scale.

3: Low temperature prototype, prototype scale.

4: Medium temperature prototype, prototype scale.

The physical characteristics of the systems at each scale (commercial and prototype) were fixed so that the results would reflect the performance of the same equipment operated under different conditions.

Shahmohammadi et al.

In addition to the four main scenarios, two sub-scenarios based on Scenario 3 (low temperature prototype) were investigated in order to assess whether the efficiency could be improved by modifying a key operating parameter. All other parameters were left the same. These sub-scenarios were:

3b: 5 bar(a) turbine discharge instead of 7.5 bar(a).

3c: NU-1000 instead of MIL-101(Cr).

The assumptions and results of the proposed hybrid system to the four case scenarios are reported in Tables 1 & 2.

Table 1 Simulation parameters -- physical characteristics. . Fixed/input variables are in blue while free/calculated variables in black.

Symbol	Description	Units	Scenario 1 Low-T Geothermal	Scenario 2 Mid-T Geothermal	Scenario 3 Low-T Prototype	Scenario 4 Mid-T Prototype	Scenario 3b 5 bar(a) turbine discharge	Scenario 3c NU-1000
	Scale		Commercial	Commercial	Demonstration	Demonstration	Demonstration	Demonstration
	Heat source fluid		Water (cp = 4.18 kJ/kg.K)					
	Heat sink fluid		Fresh cooling water (cp = 4.18 kJ/kg.K)					
	Working fluid		R134a (1,1,1,2-Tetrafluoroethane) (MW = 102.03)					
	Sorbent type*		MIL-101 (Cr) MOF (chromium (III) terephthalate), ρ_{bulk} = 250 kg/m3*					NU-1000
	Bed design		Fluidized sorption bed carousel					
	Fluidization gas		Same as working fluid with no carrier gas					
	Turbine type		Positive displacement expander with 85% isentropic efficiency					
D_b	Single bed diameter	m	1.15	1.15	0.41	0.41	0.41	0.41
H_b	Single bed packed height	m	1.0	1.0	0.91	0.91	0.91	0.91
V_b	Single bed packed volume	m³	1.04	1.04	0.12	0.12	0.12	0.12
$m_{s,bed}$	Single bed adsorbent inventory	kg	260	260	30	30	30	30
	Beds per carousel		4	4	4	4	4	4
	Number of carousels		79	13	1	1	1	1
$m_{s,T}$	Total adsorbent inventory	kg	82056	13503	118	118	118	118
	Cycle time, single step†	s	115	40	114	56	145	115

* Density of sorbent provided by Hybrixcel in Design Basis. Higher bulk densities are reported in the literature.
† The single step cycle time is the time spent in each step of the process (e.g. loaded and pre-heating). Multiply by 4 for total cycle time.

Table 2 Simulation results -- temperatures, pressures, heat flows, and mass flows. Fixed variables are in blue while free variables in black.

Symbol	Description	Units	Scenario 1 Low-T Geothermal	Scenario 2 Mid-T Geothermal	Scenario 3 Low-T Prototype	Scenario 4 Mid-T Prototype	Scenario 3b 5 bar(a) turbine discharge	Scenario 3c NU-1000
$\dot{m}_{HXH}$	Heat source flow (all carousels)	kg/s	26	26	0.20	0.20	0.20	0.20
$T_{HXH,0}$	Heat source temperature in	°C	70	225	76	225	76	76
$T_{HXH,1}$	Heat source temperature out	°C	57	146	55	162	55	56
$\dot{m}_{HXC}$	Heat sink flow (all carousels)	kg/s	26	26	0.20	0.20	0.20	0.20
$T_{HXC,0}$	Heat sink temperature in	°C	35	35	15	35	15	15
$T_{HXC,1}$	Heat sink temperature out	°C	49	115	35	97	35	34
$\dot{m}_r$	Refrigerant flow (avg, all carousels)	kg/s	0.15	0.66	0.025	0.050	0.021	0.035
$T_{H, max}$	Desorption (high) temperature (max)	°C	66	172	59	169	64	52
$T_{H, avg}$	Desorption (high) temperature (avg)	°C	62	160	55	159	59	51
$T_{L, min}$	Adsorption (low) temperature (min)	°C	39	95	29	97	24	33
$T_{L, avg}$	Adsorption (low) temperature (avg)	°C	42	103	33	104	28	35
P_{de}	Desorption pressure (avg)	bar(a)	15.5	16.8	15.9	16.6	15.6	16.2
P_{ad}	Adsorption pressure (avg)	bar(a)	7.3	5.7	6.6	5	4.1	6.2
$P_{r, 0}$	Turbine inlet pressure	bar(a)	15	15	15	15	15	15
$P_{r, 1}$	Turbine outlet pressure	bar(a)	7.5	7.5	7.5	7.5	5	7.5
L_{max}	Sorbent loading, max	wt. %*	131%	89%	141%	85%	141%	201%
L_{min}	Sorbent loading, min	wt. %*	113%	67%	117%	68%	114%	168%
f_r	Net change in refrigerant loading	wt. %	17%	22%	23%	18%	27%	33%

* Sorbent loading defined as mass of refrigerant loaded divided by mass of dry sorbent.

Table 3 Simulation results -- Energy flows and efficiencies

Symbol	Description	Units	Scenario 1 Low-T Geothermal	Scenario 2 Mid-T Geothermal	Scenario 3 Low-T Prototype	Scenario 4 Mid-T Prototype	Scenario 3b 5 bar(a) turbine discharge	Scenario 3c NU-1000
Q	Heat flow	kW	8685	8602	17.6	52.8	17.6	16.7
W_{max} (Ex)	Max. theoretical work or exergy	kW	886	3281	3.1	20.1	3.1	2.9
W	Isentropic work at turbine	kW	174	176	0.33	1.0	0.47	0.46
η_c	Max. (Carnot) efficiency	%	10.2	38.1	17.4	38.1	17.4	17.4
η_{th}	Power cycle thermal efficiency	%	2.0	2.0	1.9	1.9	2.7	2.8
η_{ex}	Power cycle exergy efficiency	%	19.6	5.4	10.9	5.0	15.2	15.8
$\eta_{turbine}$	Turbine isentropic efficiency	%	85	85	85	85	85	85
P_e	Electrical output at turbine	kWe	148	149	0.28	0.85	0.40	0.39

8. ANALYSIS AND DISCUSSION OF SIMULATION RESULTS

These simulations show that overall thermal efficiency of this system under the conditions studied is very low. There are several reasons for this, but the main reason is that most of the energy from the heat source is used to raise the temperature of the sorbent and gas (sensible heat). The sensible heat is subsequently dumped into heat sink (cooling water) during the regeneration cycle without performing useful work in the turbine. Another reason for the poor performance is that turbine operates continuously, but the columns operate in batch. Much of the cycle is spent heating and cooling, with peak pressure/flow only occurring briefly. This is partially mitigated by the use of a 4-bed carousel and the inclusion of a buffer vessel, but nevertheless the actual/average flow/pressure is less than the peak implied by the equilibrium isotherms.

Scenario 1, which is for a very low temperature differential system (TH = 76 °C, TC = 35 C), was difficult to simulate due to the very low driving force available. Scenarios 3b and 3c show that it may be possible to improve the picture by selecting a different refrigerant/sorbent pair or by operating the turbine at lower pressure.

There are several reasons why the thermal efficiency of the system is so low, many of which are related to the cyclic nature of the process. As mentioned above, one major reason is that much of the heat must go to cyclically heating then cooling the bed, which does not perform any useful work. Another source of inefficiency results from operating the turbine at a fixed inlet and outlet pressure, even though the pressure generated by the bed varies with time. Any "extra" pressure that might occur over the cycle must be throttled, and therefore does not perform any useful work. A third source of inefficiency is the inclusion of buffer tanks that act to smooth the pressure and flow of refrigerant over a cycle. The use of a positive displacement turbine is another constraint to efficiency, since they operate with a fixed volume ratio and any excess pressure is throttled and lost at the outlet.

An interesting observation from the commercial scale cases is that a tall, skinny column showed significantly more axial variation in temperature and loading than a short, fat column. This is because the refrigerant rapidly comes to equilibrium at the bottom of the column as a result of the enhanced fluidized bed kinetics, which prevents the gas from reaching the top of the column, rendering the material in the top of the column less useful. We took this into account by specifying a shorter, fatter column for the commercial-scale case. Note that a fluidized bed may be configured to reduce this effect by increasing the volumetric flow rate circulating through the bed, however it was not possible to specify this condition in Aspen Adsorption. The consequence is that the differences in temperature and loading between the top and bottom of the bed may be exaggerated in the simulation results vs. the expected performance of a high-volume circulation fluidized bed.

9. CONCLUSION

The power generation system with R134a refrigerant and both MIL-101(Cr) and NU-1000 adsorbent were studied. We modelled the adsorption isotherms from data published in the literature, assessed the viability and benefits of implementing a fluidized bed, and estimated the mass and heat transfer coefficients for a fluidized bed. Finally, a computer simulation of the process was constructed in Aspen Adsorption.

The following can be concluded from this work:

- The use of a fluidized bed in this application is appealing due to the enhanced heat and mass transfer properties of a fluidized vs. a fixed bed of solids, providing a sorbent can be developed with the required particle characteristics. We use a bubbling bed for this application.
- The fluidization of the sorbent, when designed properly and assuming 50 micron particles, is expected to consume approximately 6% of the total electrical output of the system. This is a relatively small parasitic demand and is not an impediment to this technology.
- Fluidization will require the development and manufacture of an appropriate sorbent material that meets the key performance criteria, including small particle size (< 100 micron), tight particle size distribution, high resistance to attrition, and high refrigerant loading capacity.
- It is expected that the system cycle times, and achievable refrigerant flow rates will be limited by heat transfer to / from the beds. Development efforts should therefore focus on maximizing the heat transfer coefficient and heat transfer area.
- The simulation shows that a four-bed adsorption/desorption cycle is technically feasible for both pairs of the R134a / MIL-101(Cr) and R134a/ NU1000 systems.
- Experimental data under the operating conditions assumed in this study are not publicly available. This means that we had to rely on assumptions and extrapolations that may prove to be inaccurate. The system may therefore perform significantly different than predicted by the simulation.
- The results published by PNNL appear to be based on several flawed assumptions originating from the misapplication of mathematics intended for adsorption chiller applications, which results in misleadingly optimistic predictions for a power generation cycle.

REFERENCES

[1] Moosavian SM, Rahim NA, Selvaraj J, and Solangi KH."Energy policy to promote photovoltaic generation," Renew. Sustain. Energy Rev., vol. 25, pp. 44–58, 2013.

[2] Jouhara H, Khordegah N, Almahmoud S, Delpech B, Chauhan A, Tassou SA. "Waste heat recovery technologies and applications" Therm Sci Eng Prog 2018; 6:268–89. https://doi.org/10.1016/J.TSEP.2018.04.017.

[3] Astolfi, M., Macchi, E. (2015). Efficiency correlations for axial flow turbines working with non-conventional fluids. Asme Orc 2015 (83), 1-12.

[4] Srikhirin P, Aphornratana S, Chungpaibulpatana S. "A review of absorption refrigeration technologies. Renewable and Sustainable Energy Reviews" 2001; 5(4):343 –72. doi:\bibinfo{doi}{10.1016/S1364-0321(01) 00003-X}.

[5] Jenks JJ, Motkur RK, TeGrotenhuis W, Paul BK, McGrail BP. "Simulation and Experimental Study of Metal Organic Frameworks Used in Adsorption Cooling"

[6] Jenks JJ, McGrail BP, Porter P, Motkuri R, Phillips N. "Grid Adaptive Harmonic Adsorption Recuperative Power and Cooling System" 44th Workshop on Geothermal Reservoir Engineering Stanford University, Stanford, California, February 11-13, 2019 SGP-TR-214

[7] Krzywanski J, Fan H, Feng Y, Shaikh AR, Fang M, Wang Q. Energy Conversion and Management 171, 1651 (2018)

[8] Wang, Q., Gao, X., Xu, J. Y., Maiga, A. S., & Chen, G. M. (2012). Experimental investigation on a fluidized bed adsorber/desorber for the adsorption refrigeration system. International journal of refrigeration, 35(3), 694-700.

Shahmohammadi et al.

[9] Al-Mousawi FN, Al-Dadah R, Mahmoud S. "Integrated adsorption-ORC system: Comparative study of four scenarios to generate cooling and power simultaneously" Applied Thermal Engineering 114 (2017) 1038–1052.

[10] Chorowski M, Pyrka P. 2015. "Modelling and experimental investigation of an adsorption chiller using low-temperature heat from cogeneration" Energy, 92: 221–229.

[11] Feng, Y., Hung, T., Greg, K., Zhang, Y., Li, B., Yang, J. (2015). Thermodynamic comparison between pure and mixture working fluids of organic Rankine cycles (ORCs) for low temperature waste heat recovery. Energy Conversion and Management. doi: 10.1016/j.enconman.2015.09.042